JACS
JOURNAL OF THE AMERICAN CHEMICAL SOCIETY
Article
Cite This: J. Am. Chem. Soc. XXXX, XXX, XXX−XXX
pubs.acs.org/JACS

Engineering the Substrate Specificity of a Modular Polyketide Synthase for Installation of Consecutive Non-Natural Extender Units

Edward Kalkreuter,[†,‡,∥] Jared M. CroweTipton,[†,#] Andrew N. Lowell,[⊥,¶] David H. Sherman,[⊥,§] and Gavin J. Williams*[,†,‡]

[†]Department of Chemistry, NC State University, Raleigh, North Carolina 27695, United States
[‡]Comparative Medicine Institute, NC State University, Raleigh, North Carolina 27695, United States
[⊥]Life Sciences Institute, Department of Medicinal Chemistry, University of Michigan, Ann Arbor, Michigan 48109, United States
[§]Department of Chemistry and Department of Microbiology & Immunology, University of Michigan, Ann Arbor, Michigan 48109, United States

Supporting Information

ABSTRACT: There is significant interest in diversifying the structures of polyketides to create new analogues of these bioactive molecules. This has traditionally been done by focusing on engineering the acyltransferase (AT) domains of polyketide synthases (PKSs) responsible for the incorporation of malonyl-CoA extender units. Non-natural extender units have been utilized by engineered PKSs previously; however, most of the work to date has been accomplished with ATs that are either naturally promiscuous and/or located in terminal modules lacking downstream bottlenecks. These limitations have prevented the engineering of ATs with low native promiscuity and the study of any potential gatekeeping effects by domains downstream of an engineered AT. In an effort to address this gap in PKS engineering knowledge, the substrate preferences of the final two modules of the pikromycin PKS were compared for several non-natural extender units and through active site mutagenesis. This led to engineering of the methylmalonyl-CoA specificity of both modules and inversion of their selectivity to prefer consecutive non-natural derivatives. Analysis of the product distributions of these bimodular reactions revealed unexpected metabolites resulting from gatekeeping by the downstream ketoreductase and ketosynthase domains. Despite these new bottlenecks, AT engineering provided the first full-length polyketide products incorporating two non-natural extender units. Together, this combination of tandem AT engineering and the identification of previously poorly characterized bottlenecks provides a platform for future advancements in the field.

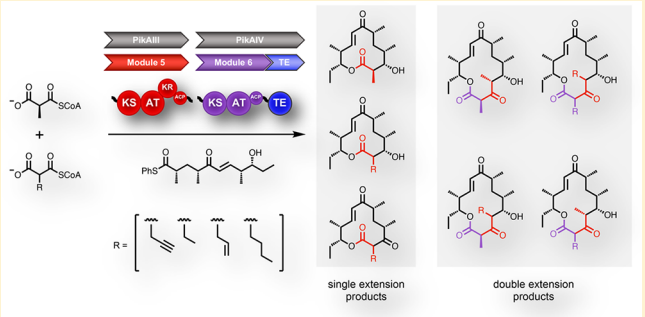

INTRODUCTION

Type I polyketide synthases (PKSs) are responsible for the biosynthesis of some of the most clinically important bioactive compounds in Nature, including the blockbuster drugs erythromycin A (antibiotic), rapamycin (immunosuppressant/anticancer), and avermectin (anthelmintic).[1] These PKSs are giant assembly line pathways that can be broken down into individual modules (Figure 1), each of which is responsible for incorporation of a single extender unit, often a coenzyme A (CoA)-linked malonate derivative. The acyltransferase (AT) within each module acts as the "gatekeeper" domain due to its innate ability to select a specific extender unit for priming of its cognate acyl carrier protein (ACP). Despite the structural diversity of polyketides, the AT domains responsible for selecting the extender units for each module typically include only three substrates: malonyl-CoA, methylmalonyl-CoA, and, to a lesser degree, ethylmalonyl-CoA.[2] Thus, except in a few rare cases, the selected substrates account for relatively narrow chemical diversity.[3−7] Instead, polyketide diversity in Nature comes from varying oxidations, cyclization patterns, or post-PKS modifications. This is represented by the four final products that result from the pikromycin (Pik) PKS (Figure 1). The development of chemoenzymatic approaches that employ non-natural malonyl-CoA analogues affords the opportunity to increase the structural diversity of polyketides by engineering PKSs.[8−10]

Traditionally, PKS engineering has focused on exchanging modules or domains to alter the final product structure, but there are three critical limitations: (1) most PKS modules incorporate natural extenders that lack useful chemical handles, (2) non-native protein−protein interactions often result in chimeras with poor catalytic efficiencies,[11,12] and (3) to achieve site-selective installation of a given non-natural extender unit into a polyketide, the specificity of the domain/module chimera must be orthogonal to that of the

Received: September 28, 2018

DOI: 10.1021/jacs.8b10521
J. Am. Chem. Soc. XXXX, XXX, XXX−XXX

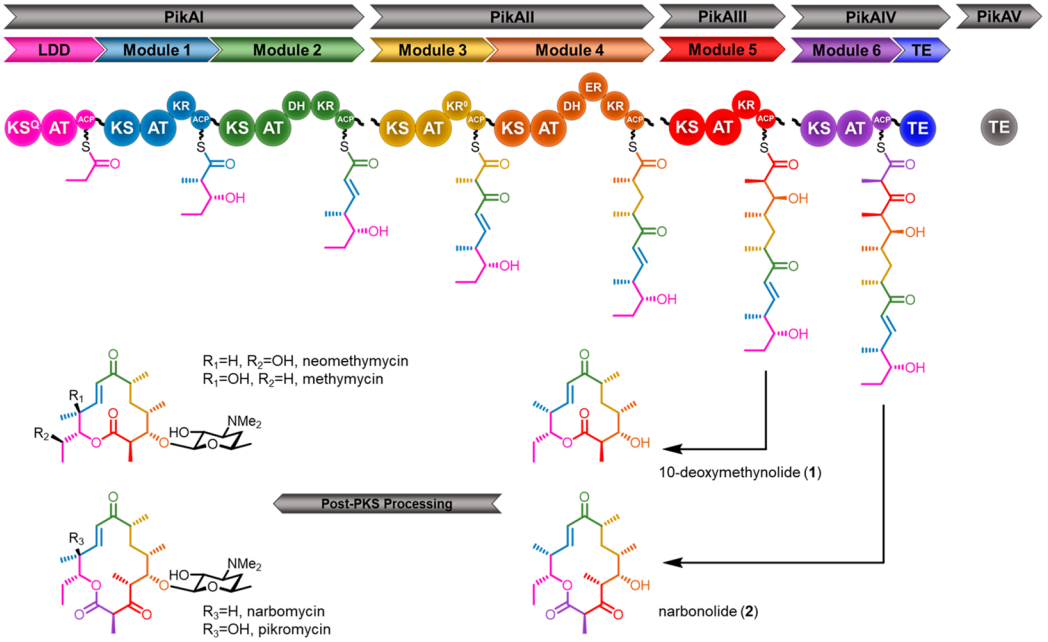

Figure 1. Pikromycin polyketide synthase and its products. ACP = acyl carrier protein; AT = acyltransferase; DH = dehydratase; ER = enoylreductase; KR = ketoreductase; KS = ketosynthase; KS^Q = ketosynthase-like decarboxylase; TE = thioesterase.

native, intact extension modules. In order to produce non-natural extender units, we and others have utilized and engineered malonyl-CoA synthetases or similar enzymes to create a panel of PKS substrates bearing a variety of useful chemical moieties.[8−10,13−15] The second issue has been approached through introduction of AT active site mutations, with varying levels of success.[9,16−19] For example, replacing the conserved YASH motif that is found in methylmalonyl-specific ATs with motifs from other natural ATs (e.g., HAFH from malonyl-CoA-specific ATs) can lead to changes in AT specificity. However, these changes alone have not completely inverted AT specificity between natural substrates and therefore do not provide the requisite orthogonality for site-selective modification of the polyketide structure.[20] In contrast, we and others have demonstrated that inherent extender unit promiscuity of some ATs provides a platform for creating new substrate specificities via site-directed mutagenesis. For example, the methylmalonyl-CoA-utilizing EryAT6 and corresponding terminal extension module (Ery6) of the 6-deoxyerythronolide B synthase (DEBS) from erythromycin A biosynthesis has significant promiscuity toward larger non-natural extender units.[21] These non-natural substrates were utilized by an engineered Ery6 module with the YASH to RASH variant, resulting in a switch from 92% methylmalonyl-CoA incorporation (wild-type enzyme) to 88% propargylmalonyl-CoA (non-natural) incorporation into the polyketide chain.[18] The ability to manipulate the substrate preference of another AT from DEBS (EryAT2) toward longer alkyl chains via a VASH motif (found in some natural ethylmalonyl-CoA-specific ATs) was also demonstrated, albeit to a lesser extent.[9] These shifts in substrate selectivity are notable and rely on the inherent promiscuity of the AT as an opportunity for redesigning substrate specificity in PKSs. Additionally, most AT engineering is accomplished with terminal extension modules that are at the end of the assembly line lacking downstream bottlenecks and involve installation of only one non-natural extender unit into the final product structure.

Herein, the ability of site-specific mutagenesis to manipulate the extender unit specificity of ATs that do not display inherent promiscuity was explored. To this end, the Pik PKS, responsible for the biosynthesis of two core macrolactones, a 12-membered 10-deoxymethynolide (10-dML, **1**) and a 14-membered narbonolide (**2**) in *Streptomyces venezuelae* ATCC 15439, was selected as a target for mutagenesis.[22] We proposed that the extension modules of this pathway would be less promiscuous toward larger extenders than the prototypical DEBS modules due to its evolution in a host that also produces ethylmalonyl-CoA and to hydrolytic proof-reading by the AT and PikAV (TEII).[23−25] Using the final two modules from this PKS, the native promiscuity of each module was first compared with a panel of natural and non-natural extender units and via a series of domain exchanges. Next, the substrate selectivity of each module was successfully engineered toward non-natural extender units via site-directed mutagenesis. Finally, a hitherto unrecognized bottleneck in PKS engineering was highlighted. To our knowledge, this is the first example of successful substrate selectivity inversion in an AT that does not belong to the prototypical DEBS assembly line. Moreover, and to the best of our knowledge, it represents the first example of two non-natural extender units being incorporated into a single full-length polyketide product.

RESULTS

Characterization of the PikAIII/PikAIV System. To date, the majority of AT substrate selectivity engineering work has been conducted in DEBS Ery6, a terminal module chosen at least in part because the fully extended non-natural chains do not need to be passed through other modules.[16−18,21,26] The Pik PKS provides a unique opportunity to probe the specificity of two adjacent monomodules that control formation of a 12- or 14-membered ring macrolactone, 10-dML (**1**) and narbonolide (**2**), respectively (Figure 1). These two enzymes are evolutionarily related, with 74% amino acid identity over two-thirds of their sequences (PikAIV lacks a KR

DOI: 10.1021/jacs.8b10521
J. Am. Chem. Soc. XXXX, XXX, XXX−XXX

Scheme 1. Bimodular Extender Unit Competition Assay[a]

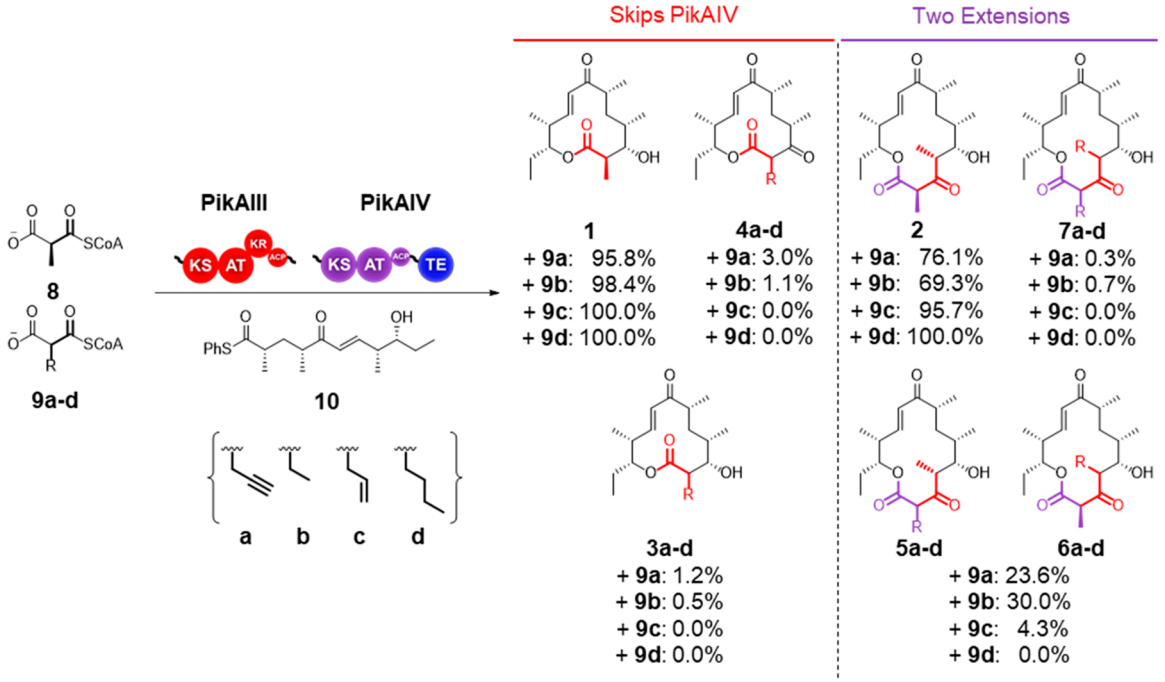

[a]The two final Pik modules are incubated with the synthetic pentaketide chain mimic **10** and a mixture of the native extender **8** and an equimolar amount of one of **9a**–**d** *in vitro*. Products **1**, **3a**–**d**, and **4a**–**d** are produced when the PikAIII-extended chain bypasses module 6 and is cyclized by the TE. Products **4a**–**d** bypass the KR domain in PikAIII. Nonreduced products derived from the native extender **8** were not observed. NADPH was produced *in situ* with an NADPH regeneration system. Product distributions shown are for the wild-type system and are calculated separately for one- and two-extension products. For all results, the standard deviation (n = 3 biological replicates) accounted for <5% of the mean value reported.

domain). Both AT domains (88% identical) utilize methylmalonyl-CoA. In contrast, the two ATs are quite dissimilar to the highly promiscuous EryAT2 (48% PikAT5, 47% PikAT6) and EryAT6 (46% PikAT5, 45% PikAT6) (Supplementary Figure S1).[9,21] To better understand substrate promiscuity beyond the DEBS ATs and to determine a baseline level of promiscuity for the Pik ATs, the modules were tested as lysates *in vitro* with **10**, a thiophenol-activated form of the natural pentaketide chain elongation intermediate and equimolar amounts of a natural (**8**) and a non-natural extender unit (e.g., **9a**, Scheme 1). The modules were prepared as lysates given that in our hands,[27] and consistent with previous reports,[28−30] module stability and reaction consistency were negatively affected by protein purification (data not shown). In this assay, pentaketide **10** is loaded onto the Cys active site of Pik KS5 for extension by one or both modules. As observed in the wild-type system (Scheme 1), after extension by PikAIII in the presence of two competing extender units, the hexaketide is transferred directly to the PikAIV TE domain, resulting in cyclization as one of two 10-dML analogues, thus "skipping" PikAIV (PikAIV does not accept the pentaketide substrate).[31] In this way, the 10-dML products must be derived from extension by PikAIII and terminated by the PikAIV TE in the absence of the second extension. Concurrently, a series of narbonolide analogues bearing variant extender units are generated by sequential extensions by PikAIII and PikAIV. Notably, a third 12-membered product (**4a**–**d**) is also possible if the non-natural elongated intermediate bypasses the PikAIII KR. These features collectively enable a precise assessment of the ability of each module to process non-natural extender units on the basis of the corresponding product distribution, which can then be readily detected and quantified by high-resolution LC-MS.[28,32]

In the native system, both modules accept only methylmalonyl-CoA (**8**), but upon incubation of the lysate with **10** and each of **9a**–**d**, the propargyl- (**9a**), ethyl- (**9b**), and allyl- (**9c**) malonyl-CoA extender units were accepted in the presence of **8** (Scheme 1 and Supplementary Tables S1 and S2). Notably though, in all cases, the non-natural single-extension products (**3a**,**b** and **4a**,**b**) made up 5% or less of the total 10-dML products, while no more than 31% of the total narbonolide product was derived from the non-natural extender unit (e.g., **5a** + **6a** + **7a**; Scheme 1). Of the three non-natural extender units that were utilized, the allyl (**9c**) was the poorest substrate, accounting for only 4.3% of the double-extension products. Regardless of the distribution of non-natural incorporation between PikAIII and PikAIV, together both modules are far less promiscuous than Ery6.[21] This narrow substrate scope provides an opportunity for expansion through mutagenesis and to explore whether inherent and extensive promiscuity is initially required for expansion via single amino acid mutations. Additionally, the discrepancy between the proportion of single- and double-extension products derived from the non-natural extender unit posed questions about promiscuity of individual modules within the same PKS. Furthermore, detection of new keto-10-dML products (**4a**,**b**, *vide infra*) raised the issue of processing efficiency by downstream domains.

Comparison of the Pikromycin PKS Acyltransferases. There are three gatekeeping domains potentially responsible for the low production of **3a**–**d**/**4a**–**d** by the modular Pik system: (1) the Pik AT5, (2) the downstream ketosynthase Pik

DOI: 10.1021/jacs.8b10521
J. Am. Chem. Soc. XXXX, XXX, XXX−XXX

KS6, or (3) the Pik TE. Several chimeric modules were subsequently designed to probe the role of the AT domains in determining the observed product profile. The native AT of PikAIV was substituted with PikAT5 (R2, Figure 2), and the

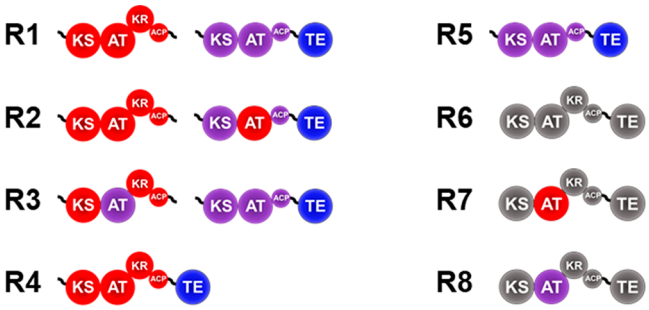

Figure 2. Wild-type and chimeric module systems designed to probe the specificity of each AT from PikAIII and PikAIV. R1 is the wild-type PikAIII (red) and wild-type PikAIV (purple) with the native PikAIV TE (blue). AT swaps were used to create R2 and R3 from R1. R4 is PikAIII fused to the PikAIV TE. Each Pik AT was swapped into Ery6TE (R6, gray) to generate R7 and R8.

native AT of PikAIII was substituted with PikAT6 (R3, Figure 2). In both of these chimeras, newly defined boundaries were used[33] but nevertheless resulted in less total product compared to the wild-type system, with the R2 chimera less than a tenth as active as the wild-type system (Table 1, Supplementary Table S3, and Supplementary Figure 2). As expected, based upon the assumption that the terminal AT (Pik AT6) was more promiscuous than those upstream, the chimera that contained two Pik AT5 domains, R2, produced almost 25% less propargyl **5a**/**6a** products than the wild-type system (R2, Table 1). Consistent with these results, the system containing two Pik AT6 domains, R3, produced more than 15-fold higher levels of propargyl **3a**/**4a** and 1.6-fold more **5a**/**6a** products than the wild-type system (R3, Table 1). Together, these data indicate that Pik AT6 is significantly more promiscuous than Pik AT5 and that this feature may contribute to the low production of **3a**–**d**/**4a**–**d** by the wild-type system.

Table 1. Product Distributions Catalyzed by Domain Swapped Chimeras

	10-dML[a]	narbonolide[b]		
enzyme	**3a** + **4a**	**5a** + **6a**	**7a**	relative activity[c]
R1	4.2%[d]	23.6%[d]	0.3%[d]	100.0[d]
R2	11.8%[d]	17.9%[d]	0.2%[d]	9.0[d]
R3	66.7%[d]	37.2%[d]	0.6%[d]	47.5[d]
R4	0.8%[d]	[f]	[f]	100.0[d]
R5	N.D.[e]	[f]	[f]	N.D.[e]
R6	7.4%[d]	[f]	[f]	586.0[d]
R7	7.2%[d]	[f]	[f]	180.3[d]
R8	N.D.[e]	[f]	[f]	N.D.[e]

[a]Percent of **3a** + **4a** out of all 10-dML products (**1**, **3a**, and **4a**). See Scheme 1 for structures of products. [b]Percent of (**5a** + **6a**) or **7a** out of all narbonolide products (**2**, **5a**, **6a**, and **7a**). See Scheme 1 for structures of products. [c]Total activity of each system relative to R1 (for bimodular systems) or R4 (for monomodular systems) is based on total amount of products for each reaction (sum of **1**, **2**, **3a**, **4a**, **5a**, **6a**, and **7a**). [d]The standard deviation (n = 3 biological replicates) accounted for <5% of the mean value reported. [e]N.D. = not detected. [f]Not applicable.

Interestingly, only 0.6% of the double-extension product from R3 contained two propargyls (**7a**) even though 66% of the single-extension products (**3a** + **4a**) are derived from the propargyl extender (Table 1). However, upon closer examination, 99% of the 10-dML single-extension products was the unreduced propargyl 10-dML analogue **4a** (Supplementary Table S3). The discrepancy between the portion of single and double propargyl products could be due to the native screening ability of Pik KR5[34] and/or to perturbations in the KR due to the impaired function of the PKS AT domain chimera. However, with the natural extender unit **8**, only the 10-dML product (**1**; bearing C-3 OH) is observed (Scheme 1), suggesting that the native processing ability of Pik KR5 is at least dependent on the extender unit C2 side-chain. As mass ions consistent with a keto-narbonolide product were not found (Scheme 1), it is likely that Pik KS6 fails to process C-3 keto hexaketide chains.

To account for any substrate bias by domains within PikAIV that impact product distributions, particularly the KS, PikAIII and PikAIV were decoupled by fusing PikAIII to the Pik TE. In addition to substrate competition assays with both modules (Scheme 1), this now enables competition assays with PikAIII-TE alone (Scheme 2), though not PikAIV alone, as it does not accept the pentaketide substrate **10**. As expected for a single-extension module, PikAIII-TE produced only 10-dML-like products, and narbonolides were not detected. Notably though, of these products, only 0.8% were derived from the propargyl extender unit, with half of these comprising the corresponding keto-10-dML product **4a** (Scheme 2 and Table 1, R4). By comparison, 4.2% of the 10-dML products were derived from the propargyl extender unit when the wild-type bimodular system was used (Table 1, R1). Given that the ratio of propargyl product from R4 was no higher than that with the wild-type bimodular system, this result suggests that the lack of extender unit promiscuity displayed by PikAIII is likely due to PikAIII itself and not due to downstream gatekeeping by components of PikAIV, with the possible exception of the TE.[27,35]

Finally, to determine the possible effect of the domains surrounding the AT within each module, each of the two Pik ATs was introduced into Ery6-TE (R6, Figure 2), a module and TE pair known to be capable of producing high yields of non-natural 10-dML products,[18] yielding the chimeras R7 and R8 (Figure 2). Once again, issues with chimera stability prevented a direct comparison of the two ATs in these chimeras, as Ery6TE_PikAT6 (R8) was completely inactive (Table 1). However, the Ery6-TE_PikAT5 (R7) construct had a significantly more relaxed substrate selectivity (7.2% **3a**/**4a**) than did PikAIII-TE (0.8% **3a**/**4a**) and nearly equal to that of wild-type Ery6-TE (7.4% **3a**/**4a**) (Table 1). This 9-fold increase in propargyl incorporation by PikAT5 when substituted into Ery6-TE from its native module, along with the results of the other three domain swaps establishes the importance both of AT substrate selection and of the substrate promiscuity of the other post-AT domains, especially the KS and the KR.

Effects of Active Site Mutations on Extender Unit Incorporation. In addition to the insight into substrate incorporation, the domain swaps also highlighted two other aspects important for PKS engineering. First, even with the recently updated AT boundaries,[33] domain exchanging often results in inactive or poorly active enzymes. Second, some modules, regardless of AT selectivity, are naturally more

DOI: 10.1021/jacs.8b10521
J. Am. Chem. Soc. XXXX, XXX, XXX−XXX

Scheme 2. Single Module Extender Unit Competition Assay[a]

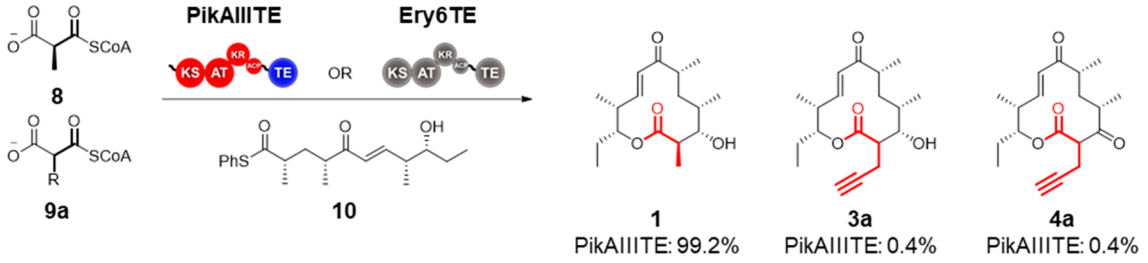

[a]The fusion protein PikAIII-TE or the final module of the DEBS PKS, Ery6TE, is incubated with the synthetic pentaketide chain mimic **10** and a mixture of the native extender **8** and an equimolar amount of **9a** *in vitro*. NADPH was produced *in situ* with an NADPH regeneration system. For all results, the standard deviation (n = 3 biological replicates) accounted for <5% of the mean value reported. Percentages are shown for wild-type systems.

Table 2. Product Distributions Catalyzed by Engineered Mono- and Bimodular Pik Systems

	enzyme			10-dML[a]	narbonolide[b]		
entry	PikAIII-TE	PikAIII	PikAIV	**3a** + **4a**	**5a** + **6a**	**7a**	relative activity[c]
R9	WT	[d]	[d]	0.8%[e]	[d]	[d]	100.0[e]
R10	V753A	[d]	[d]	21.1%[e]	[d]	[d]	4.2[e]
R11	Y755R	[d]	[d]	N.D.[f]	[d]	[d]	N.D.[f]
R12	Y755V	[d]	[d]	42.2%[e]	[d]	[d]	81.5[e]
R13	WT (*apo*)	[d]	[d]	N.D.[f]	[d]	[d]	N.D.[f]
R14	[d]	WT	WT	4.2%[e]	23.6%[e]	0.3%[e]	100.0[e]
R15	[d]	V753A	WT	7.7%[e]	21.3%[e]	0.8%[e]	92.5[e]
R16	[d]	Y755V	WT	55.9%[e]	61.9%[e]	16.7%[e]	82.1[e]
R17	[d]	WT	Y753V	4.4%[e]	77.2%[e]	1.3%[e]	86.8[e]
R18	[d]	Y755V	Y753V	44.6%[e]	59.6%[e]	14.7%[e]	51.7[e]
R19	[d]	WT (*apo*)	WT (*apo*)	N.D.[f]	N.D.[f]	N.D.[f]	N.D.[f]

[a]Percent of **3a** + **4a** out of all 10-dML products (**1**, **3a**, and **4a**). See Scheme 1 for structures of products. [b]Percent of (**5a** + **6a**) or **7a** out of all narbonolide products (**2**, **5a**, **6a**, and **7a**). See Scheme 1 for structures of products. [c]Total activity of each system relative to R9 (for monomodular systems) or R14 (for bimodular systems) is based on total amount of products (sum of **1**, **2**, **3a**, **4a**, **5a**, **6a**, and **7a**). [d]Not applicable. [e]The standard deviation (n = 3 biological replicates) accounted for <5% of the mean value reported. [f]N.D. = not detected.

substrate-permissive.[9,15,32] To circumvent the first issue and take advantage of the second, AT active site mutagenesis could be utilized for maximum engineering efficiency.

By inspection of homology models created for PikAT5 and PikAT6, there appears to be no significant structural differences between the two active sites that could otherwise explain the difference in extender unit promiscuity and guide mutagenesis efforts (Supplementary Figure S4). Indeed, as indicated by amino acid sequence alignments and the homology models, both ATs also share many of the same active site residues as EryAT6, including the YASH motif (Supplementary Figures S1 and S4). Given that the structural features that explain the observed difference in extender unit promiscuity of PikAT5 and PikAT6 might be subtle and could not be detected by homology modeling, we set out to identify mutations that could impact the specificity. Twenty mutants, spanning mutations at nine active site residues in AT5 of PikAIII-TE, were first tested with the pentaketide **10** and a mixture of extender units, **8**/**9a** (Supplementary Table S4). This preliminary set, including the two best characterized mutations from EryAT6, V742A and Y744R (Ery6TE numbering), was introduced into PikAIII-TE[17,18] Analysis of the distribution of **1**/**3a** supported by each PikAIII-TE mutant revealed that, surprisingly, Y755R resulted in a completely inactive enzyme in contrast to the flip in selectivity observed in Ery6TE (Supplementary Table S4).[18] The V753A mutation, on the other hand, did support improved production of **3a** compared to the wild-type enzyme. Accordingly, the product distributions of V753A and Y755R were analyzed in more detail. In this single module system, **3a**/**4a** production increased 26-fold upon introduction of the mutation V753A, as judged by the relative amount of **3a**/**4a** vs the methyl product, **1** (R10, Table 2). As anticipated, no other products were detected with Y755R (R11, Table 2), while the apo version of the wild-type enzyme was also completely inactive (R13, Table 2).

To explore why the Tyr → Arg mutation is effective in one methyl-specific AT (EryAT6) but not in the Pik ATs, molecular dynamics (MD) simulations were utilized with EryAT6 and PikAT6 homology models (Supplementary Figure S3). In EryAT6, Arg744 forms a salt bridge with the neighboring Asp743, which in turn competes in another salt bridge with Arg674 (Figure 3A). According to the MD simulations, both arginines also interact with Asp613, facilitating distribution of the positive charge and also maintaining integrity of the active site. In the MD simulation of PikAT6 Y753R, Arg753 appears to extend into the active site rather than forming salt bridges as seen in DEBS. Arg674 in EryAT6 has been replaced with Ala683 in PikAT6, which in turn interacts with the hydrophobic Val621 in place of Asp613 in EryAT6 (Figure 3B). Accordingly, compared to EryAT6, the predicted nonpolar environment in the PikAT6 active site is not as suitable for accepting the substrate of the engineered Arg753, and the distance between the two catalytic residues

DOI: 10.1021/jacs.8b10521
J. Am. Chem. Soc. XXXX, XXX, XXX−XXX

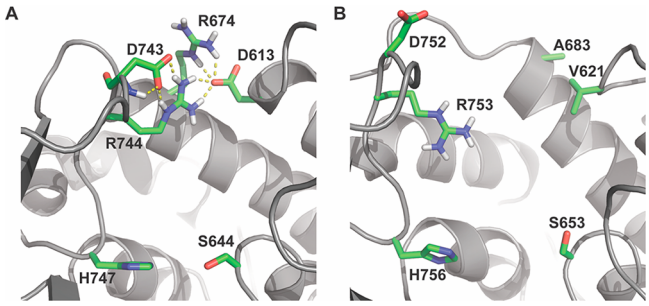

Figure 3. Models of (A) EryAT6 Y744R and (B) PikAT6 Y753R ATs after undergoing MD simulations. Distances between catalytic residues in the mutant EryAT6 (4.8 Å) are long but catalytically competent. The same distance in the mutant PikAT6 (8.4 Å) is characteristic of an inactive AT domain.

widens commensurately (8.4 Å in PikAT6 Y753R vs 4.8 Å in EryAT6 Y744R). This distance would be too far to maintain the interactions between Ser653 and His756 necessary for catalytic activity.

Given the MD simulations and that Y755R resulted in an inactive PikAIII-TE, the corresponding Tyr → Val sequence variation shared between many ethylmalonyl-CoA-specific ATs was introduced into PikAIII-TE (R12, Table 2).[36] This mutation, which has also recently been introduced into EryAT2,[9] resulted in a significantly more promiscuous module with nearly half of the products derived from **9a**. Next, both functional mutations were introduced into PikAIII and PikAIV and assayed as part of a bimodular system (R14–R19, Table 2). The Val → Ala mutation in PikAIII resulted in a more modest formation of the propargyl products (**3a**, **4a**, and **7a**) compared to the wild-type bimodular system (R15, Table 2); however, the Tyr → Val mutation in either module flipped the selectivity of the bimodular system, preferring the non-natural substrate **9a** over the natural substrate **8**, as judged by the ratio of narbonolide products **2**, **5a**/**6a**, and **7a**, e.g., 21.4% **2**, 61.9% **5a**/**6a**, and 16.7% **7a** (R16, Table 2). With PikAIII Y755V, a 13-fold increase in preference for propargyl was observed in the single extension product compared with the wild-type bimodular system, but unlike with the unstable chimera R3, 90% of the product was reduced (R16 and R14, respectively, Supplementary Table S3). Subsequently, whereas the wild-type bimodular system only supports production of 0.3% dipropargyl narbonolides, nearly 17% of the narbonolides formed by PikAIII Y755V are derived from two propargyl extender units (**7a**). This successful selectivity shift demonstrates that even with other domains potentially impacting substrate selection (e.g., KS, KR, and/or TE), even the most stringent of systems can be engineered to accept a desired new substrate.

The PikAIII Y755V/PikAIV Y753V system was also probed for substrate tolerance beyond methyl and propargyl by including either ethyl-, allyl-, or butylmalonyl-CoA in equimolar concentrations with methylmalonyl-CoA (Table 3, Supplementary Table S2, and Supplementary Figure 4). As desired, the double mutant system showed improved activity with all three additional non-natural substrates tested. For ethyl, the non-natural narbonolide products were also more abundant than the native product **2**. Gratifyingly, the allyl and butyl extenders that were not accepted to any degree by wild-type PikAIII (or even by the more promiscuous PikAIV for butyl) were accepted by both mutant modules, even resulting

Table 3. Product Distributions Catalyzed by the Double Mutant Bimodular Pik System with Non-Natural Extender Units[a]

	PikAIII Y755V + PikAIV Y753V			
	10-dML[a]		narbonolide[b]	
extender unit	**3a–d**	**4a–d**	**5a–d** + **6a–d**	**7a–d**
propargyl (**a**)	41.0%[c] (10.6)[d]	3.6%[c]	59.6%[c] (2.5)[d]	14.7%[c] (49.0)[d]
ethyl (**b**)	8.0%[c] (6.1)[d]	1.8%[c]	49.1%[c] (1.6)[d]	17.4%[c] (24.9)[d]
allyl (**c**)	3.7%[c] (>8000)[d]	4.3%[c]	16.7%[c] (3.9)[d]	3.3%[c] (>3300)[d]
butyl (**d**)	N.D. (>11 300)[d]	11.3%[c]	5.4%[c] (>5400)[d]	N.D.[e] [f]

[a]Percent of **3a–d** or **4a–d** out of all 10-dML products (**1**, **3a–d**, and **4a–d**). [b]Percent of (**5a–d** + **6a–d**) or **7a–d** out of all narbonolide products (**2**, **5a–d**, **6a–d**, and **7a–d**). [c]The standard deviation (n = 3 biological replicates) accounted for <5% of the mean value reported. [d]Fold increase calculated based on values from the wild-type system in Scheme 1. In the case of a product that was not detected with the wild-type enzyme, the fold increase was calculated based on the limit of detection, 0.001% of total products. [e]N.D. = not detected. [f]Not applicable.

in the double allyl product **7c**, albeit in reduced percentage yields as compared to the propargyl and ethyl products. This is particularly interesting given that non-natural narbonolide products were not produced with an engineered bimodular DEBS system.[18] The differences in activities between substrates is notable, especially with the two C3 substrates, propargyl (**9a**, robust) and allyl (**9c**, poor), in both the wild-type (Scheme 1) and mutant (Table 3) systems. The primary difference between the two substrates that might explain their disparate activities with PikAIII/PikAIV is their relative flexibilities, whereby the rigid propargyl side-chain can orient toward the rear of the active site, while the more flexible allyl side-chain could clash more with the YASH motif, even with residues that lie beyond Tyr755 targeted in this study.

As with the propargyl extender, each non-natural substrate resulted in significant production of the unreduced 10-dML products, especially in the cases of allyl and butyl, where greater than half of the single-extension products were the unreduced **4c** and **4d** products (Table 3 and Supplementary Table S3). In fact, none of the single-extension butyl product was reduced by the KR, preventing production of any double-butyl narbonolide product likely due to the downstream PikKS6 discriminating against chains with the non-native oxidation pattern. This additional gatekeeping by the KR and KS sets the stage for further engineering in nonterminal PKS modules.

DISCUSSION

PKSs provide the ability to template a series of reactions in order to achieve a desired product, with each module responsible for recruitment of a single extender unit into the polyketide scaffold. However, the envisioned goal of being able to stitch together any domain or module seamlessly still cannot be attained without significant loss in enzyme function,[11,33,37] likely due to delicate protein:protein interactions that are faulty in chimeric PKSs and prevent proper vectoral biosynthesis.[38,39] In this study, even with two ATs sharing 88% identity, the AT exchanges resulted in vastly different enzyme activity levels.

DOI: 10.1021/jacs.8b10521
J. Am. Chem. Soc. XXXX, XXX, XXX–XXX

Rather than directly addressing the impact of AT exchanges, which has been well documented previously,[11,40−42] the chimeras were used to identify the source of extender unit selectivity in the pikromycin PKS. Instead, to realize the potential of PKS engineering, site-specific mutations can be introduced to shift selectivity toward or away from a given substrate.

Herein, two very similar ATs from the pikromycin PKS were compared with each other and with the well-characterized EryAT6. Despite these three ATs sharing all residues known or predicted to influence substrate selectivity, they exhibit very different levels of substrate promiscuity. Additionally, mutations that cause a substrate selectivity flip in EryAT6 (Y744R) result in inactive enzymes in the Pik ATs. In other cases, such as with the Tyr → Val mutation explored here, the mutation results in a shift toward larger extenders, demonstrating that an AT with as little native promiscuity as PikAT5 can be engineered to prefer non-natural substrates (4.2% **3a**/**4a** to 55.9% **3a**/**4a**, R14 and R16, Table 2).

In its native setting, PikAIV accounted for the clear majority of non-natural extender unit incorporation by the bimodular system. Through AT exchanges and mutagenesis, much of this discrepancy in promiscuity between PikAIII and PikAIV was shown to locate with the ATs themselves; however, as demonstrated by the 9-fold change in percent propargyl product for two PikAT5-containing modules (R4 and R7, Table 1) and the significant discrimination by PikKR5 against larger extenders (Table 3), the surrounding domains play a significant role in the distribution of natural vs non-natural products. The effect of the KR is especially notable regarding the incorporation of non-natural extender units, especially as the extenders become larger (e.g., butyl). As the selectivity of the AT is altered, the ketoreductase (and potentially other domains) will need to be exchanged or engineered to be compatible with the desired product. As engineering of these domains progresses, larger and more exotic extenders can be used to further push the limits of these modular assembly line-like enzymes.

Cumulatively, site-specific mutagenesis of PikAT5 and PikAT6 has led to robust yields of the first full-length polyketide with two non-natural extenders and to the first nonterminal methyl-specific module to accept and process a non-natural extender unit. Subsequently, this work significantly expands the synthetic potential of engineered PKSs and opens up new avenues for engineering other systems. Additionally, the new 10-dML and narbonolide analogues reported herein can be further derivatized through semisynthetic chemistry, especially "click chemistry".

MATERIALS AND METHODS

General Information. Materials and reagents were purchased from Sigma-Aldrich (St. Louis, MO, USA) unless otherwise noted. Isopropyl β-D-thioglactoside (IPTG) was purchased from Calbiochem (Gibbstown, NJ, USA). The *E. coli* BAP1 strain was provided by Dr. Blaine Pfeifer at the University at Buffalo.[43] Construction of the Ery6TE-pET28 plasmid was described previously.[18] All module sequences are listed in Supplementary Table S5. Primers were purchased from Integrated DNA Technologies (Coralville, IA, USA). All *holo* proteins were expressed in BAP1 cells, and all *apo* proteins were expressed in *E. coli* BL21 (DE3) cells. All primers are listed in Supplementary Table S6.

Lysate Preparation. Modules (wild-type and mutant PikAIII-(TE), wild-type and mutant PikAIV, and wild-type and mutant Ery6TE) were expressed overnight at 16 °C in 300 mL cultures of LB media with the appropriate antibiotics. Protein production was induced with 1 mM IPTG at an OD_{600} of 0.6. After overnight expression, the culture was centrifuged at 4700 rpm for 20 min, and the supernatant was discarded. The cells were resuspended in 1 mL of module storage buffer (100 mM sodium phosphate, pH 7.4, 1 mM EDTA, 1 mM tris(2-carboxyethyl)phosphine (TCEP), 20% v/v glycerol, 0.1 μL of Benzonase (NEB), and EDTA-free protease inhibitor cocktail (Roche, Basel, CH)) and sonicated using 51% amplitude, 10 s on, 20 s off for 10 min. After sonication, the lysed cells were centrifuged at 18 000 rpm for 1 h. The lysates were aliquoted and stored at −80 °C. Protein purity was verified by SDS-PAGE. Protein quantification was carried out using the Bradford protein assay kit from Bio-Rad.

MatB Reactions and acyl-CoA Preparation. Wild-type and mutant T207G/M306I MatB were purified, and 8 mM malonyl-CoA (**8**, **9a**−**d**) stocks were set up as previously disclosed[10] and described in the Supplemental Methods.

Pentaketide Assay. The pentaketide assay was set up with a total volume of 80 μL in 100 mM sodium phosphate, pH 7.0, and 2 mM $MgCl_2$. The reaction conditions included 1 mM TP-pentaketide (**10**), 1.75 mM of each competing malonyl-CoA from MatB reactions (**8**, **9a**−**d**), an NADPH regeneration system (5 mM glucose-6-phosphate, 500 μM $NADP^+$, and 0.008 U/mL glucose-6-phosphate dehydrogenase), and lysate containing the module or modules. For the bimodular reactions, the proteins were included as a total of 29.4 μL of lysate, at a final concentration of 1−3 μM. Module concentrations were calculated by Bradford assay and SDS-PAGE gel analysis, and results were normalized based on protein content for each reaction. Negative controls (R13 and R19) were run with *apo* modules lacking the phosphopantetheine modifications on the ACP domains. Reactions proceeded at room temperature for 16 h and were quenched with an equal volume of −20 °C methanol. After quenching, all reactions were centrifuged at 13 300 rpm three times for 3 h total, and the supernatant was filtered through a nylon 0.2 μm filter. Analysis was carried out on a high-resolution mass spectrometer (ThermoFisher Scientific Exactive Plus MS, a benchtop full-scan Orbitrap mass spectrometer) using heated electrospray ionization . The sample was analyzed via LC-MS injection into the mass spectrometer at a flow rate of 225 μL/min. The mobile phase B was acetonitrile with 0.1% formic acid, and mobile phase A was water with 0.1% formic acid (see Table S7 for gradient and scan parameters). The mass spectrometer was operated in positive ion mode. The LC column was a Thermo Hypersil Gold 50 × 2.1 mm, 1.9 μm particle size. This assay produces 10-dML and narbonolide products that can be seen as their $[M + H]^+$, $[M + H - H_2O]^+$, and $[M + Na]^+$ ions and keto-10-dML products that can be seen as their $[M + H]^+$ and $[M + Na]^+$ ions. Extracted ions for each listed ion were summed for comparison purposes. For retention times, calculated masses, observed masses, representative extracted ion counts, and representative chromatograms, see Tables S1, S2, and S4 and Figures S2 and S5.

Homology Models and Molecular Dynamics. Wild-type homology models for EryAT6, PikAT5, and PikAT6 were created using the I-TASSER online server.[44−46] Mutations were introduced into structurally converged wild-type models with Discovery Studio 4.1 from Accelrys Software, Inc. (San Diego, CA, USA). Molecular graphics and analyses of MD trajectories and PDB snapshots were performed with VMD 1.9.2 and UCSF Chimera 1.10.1.[47−49] Further analysis was performed with CPPTRAJ.[50] Images were rendered with POV-Ray.[51]

Using the AMBER14 software package, individual models' charges were neutralized with sodium ions in Xleap.[52] All models were then solvated with a 15 Å buffer of TIP3P water, also within Xleap. The enzymes and substrates were parametrized with ff12SB and GAFF force fields from the AMBER14 software package. Prior to production MD simulations, solvated systems were treated with four heating and seven minimization steps. Steps 2, 3, 5, and 11 heated the system to 300 K over times of 20−100 ps each. The first nine steps held the protein fixed, with the restraint constant being lowered each step. Steps 10 and 11 used no restraints. Minimization steps were completed when the change in the root-mean-square was below

DOI: 10.1021/jacs.8b10521
J. Am. Chem. Soc. XXXX, XXX, XXX−XXX

0.01 kcal/mol·Å for the first two minimization steps and below 0.001 kcal/mol·Å for the remaining minimizations. Production simulations lasted between 10 and 60 ns for each model. Step times were 2 fs. The nonbonded interaction cutoff was imposed at 9.0 Å. For the two mutants, models were based on the simulated wild-type enzymes (Supplementary Figure S3).

■ ASSOCIATED CONTENT

Supporting Information

The Supporting Information is available free of charge on the ACS Publications website at DOI: 10.1021/jacs.8b10521.

Supplementary tables, supplemental figures, and detailed methods that describe site-directed mutagenesis of modules, construction of chimeras, expression and purification of wild-type and mutant MatB, and synthesis of acyl-CoAs by MatB (PDF)

■ AUTHOR INFORMATION

Corresponding Author

*gjwillia@ncsu.edu

ORCID

Andrew N. Lowell: 0000-0001-5357-5279
David H. Sherman: 0000-0001-8334-3647
Gavin J. Williams: 0000-0003-2172-9063

Present Addresses

[‖]Department of Chemistry, The Scripps Research Institute, Jupiter, Florida 33458, United States.
[#]Nephron Pharmaceuticals Corporation, West Columbia, South Carolina 29172, United States.
[¶]Department of Chemistry, Virginia Tech, Blacksburg, Virginia 24061, United States.

Notes

The authors declare no competing financial interest.

■ ACKNOWLEDGMENTS

This study was supported in part by National Institutes of Health grants GM104258 (G.J.W.), GM118101 (D.H.S.), and GM076477 (D.H.S.) and the Hans W. Vahlteich Professorship (D.H.S.). All high-resolution LC-MS measurements were made in the Molecular Education, Technology, and Research Innovation Center (METRIC) at NC State University.

■ REFERENCES

(1) Wang, H.; Fewer, D. P.; Holm, L.; Rouhiainen, L.; Sivonen, K. Atlas of nonribosomal peptide and polyketide biosynthetic pathways reveals common occurrence of nonmodular enzymes. *Proc. Natl. Acad. Sci. U. S. A.* **2014**, *111* (25), 9259−9264.

(2) Chan, Y. A.; Thomas, M. G. Formation and characterization of acyl carrier protein-linked polyketide synthase extender units. *Methods Enzymol.* **2009**, *459*, 143−63.

(3) Chan, Y. A.; Boyne, M. T., 2nd; Podevels, A. M.; Klimowicz, A. K.; Handelsman, J.; Kelleher, N. L.; Thomas, M. G. Hydroxymalonyl-acyl carrier protein (ACP) and aminomalonyl-ACP are two additional type I polyketide synthase extender units. *Proc. Natl. Acad. Sci. U. S. A.* **2006**, *103* (39), 14349−14354.

(4) Mo, S.; Kim, D. H.; Lee, J. H.; Park, J. W.; Basnet, D. B.; Ban, Y. H.; Yoo, Y. J.; Chen, S. W.; Park, S. R.; Choi, E. A.; Kim, E.; Jin, Y. Y.; Lee, S. K.; Park, J. Y.; Liu, Y.; Lee, M. O.; Lee, K. S.; Kim, S. J.; Kim, D.; Park, B. C.; Lee, S. G.; Kwon, H. J.; Suh, J. W.; Moore, B. S.; Lim, S. K.; Yoon, Y. J. Biosynthesis of the allylmalonyl-CoA extender unit for the FK506 polyketide synthase proceeds through a dedicated polyketide synthase and facilitates the mutasynthesis of analogues. *J. Am. Chem. Soc.* **2011**, *133* (4), 976−85.

(5) Chang, C.; Huang, R.; Yan, Y.; Ma, H.; Dai, Z.; Zhang, B.; Deng, Z.; Liu, W.; Qu, X. Uncovering the formation and selection of benzylmalonyl-CoA from the biosynthesis of splenocin and enterocin reveals a versatile way to introduce amino acids into polyketide carbon scaffolds. *J. Am. Chem. Soc.* **2015**, *137* (12), 4183−90.

(6) Yoo, H. G.; Kwon, S. Y.; Kim, S.; Karki, S.; Park, Z. Y.; Kwon, H. J. Characterization of 2-octenoyl-CoA carboxylase/reductase utilizing pteB from *Streptomyce avermitilis*. *Biosci., Biotechnol., Biochem.* **2011**, *75* (6), 1191−3.

(7) Eustáquio, A. S.; McGlinchey, R. P.; Liu, Y.; Hazzard, C.; Beer, L. L.; Florova, G.; Alhamadsheh, M. M.; Lechner, A.; Kale, A. J.; Kobayashi, Y.; Reynolds, K. A.; Moore, B. S. Biosynthesis of the salinosporamide A polyketide synthase substrate chloroethylmalonyl-coenzyme A from *S*-adenosyl-L-methionine. *Proc. Natl. Acad. Sci. U. S. A.* **2009**, *106* (30), 12295−12300.

(8) Koryakina, I.; Williams, G. J. Mutant malonyl-CoA synthetases with altered specificity for polyketide synthase extender unit generation. *ChemBioChem* **2011**, *12* (15), 2289−2293.

(9) Vogeli, B.; Geyer, K.; Gerlinger, P. D.; Benkstein, S.; Cortina, N. S.; Erb, T. J. Combining promiscuous acyl-CoA oxidase and enoyl-CoA carboxylase/reductases for atypical polyketide extender unit biosynthesis. *Cell Chem. Biol.* **2018**, *25* (7), 833−839.

(10) Koryakina, I.; McArthur, J.; Randall, S.; Draelos, M. M.; Musiol, E. M.; Muddiman, D. C.; Weber, T.; Williams, G. J. Poly specific trans-acyltransferase machinery revealed via engineered acyl-CoA synthetases. *ACS Chem. Biol.* **2013**, *8*, 200−208.

(11) McDaniel, R.; Thamchaipenet, A.; Gustafsson, C.; Fu, H.; Betlach, M.; Ashley, G. Multiple genetic modifications of the erythromycin polyketide synthase to produce a library of novel "unnatural" natural products. *Proc. Natl. Acad. Sci. U. S. A.* **1999**, *96* (5), 1846−51.

(12) Chan, Y. A.; Podevels, A. M.; Kevany, B. M.; Thomas, M. G. Biosynthesis of polyketide synthase extender units. *Nat. Prod. Rep.* **2009**, *26* (1), 90.

(13) Ad, O.; Thuronyi, B. W.; Chang, M. C. Y. Elucidating the mechanism of fluorinated extender unit loading for improved production of fluorine-containing polyketides. *Proc. Natl. Acad. Sci. U. S. A.* **2017**, *114* (5), E660−E668.

(14) Musiol-Kroll, E. M.; Zubeil, F.; Schafhauser, T.; Hartner, T.; Kulik, A.; McArthur, J.; Koryakina, I.; Wohlleben, W.; Grond, S.; Williams, G. J.; Lee, S. Y.; Weber, T. Polyketide bioderivatization using the promiscuous acyltransferase KirCII. *ACS Synth. Biol.* **2017**, *6* (3), 421−427.

(15) Möller, D.; Kushnir, S.; Grote, M.; Ismail-Ali, A.; Koopmans, K. R. M.; Calo, F.; Heinrich, S.; Diehl, B.; Schulz, F. Flexible enzymatic activation of artificial polyketide extender units by *Streptomyces cinnamonensis* into the monensin biosynthetic pathway. *Lett. Appl. Microbiol.* **2018**, *67* (3), 226−234.

(16) Bravo-Rodriguez, K.; Klopries, S.; Koopmans, K. R.; Sundermann, U.; Yahiaoui, S.; Arens, J.; Kushnir, S.; Schulz, F.; Sanchez-Garcia, E. Substrate flexibility of a mutated acyltransferase domain and implications for polyketide biosynthesis. *Chem. Biol.* **2015**, *22* (11), 1425−30.

(17) Sundermann, U.; Bravo-Rodriguez, K.; Klopries, S.; Kushnir, S.; Gomez, H.; Sanchez-Garcia, E.; Schulz, F. Enzyme-directed mutasynthesis: a combined experimental and theoretical approach to substrate recognition of a polyketide synthase. *ACS Chem. Biol.* **2013**, *8*, 443−450.

(18) Koryakina, I.; Kasey, C.; McArthur, J. B.; Lowell, A. N.; Chemler, J. A.; Li, S.; Hansen, D. A.; Sherman, D. H.; Williams, G. J. Inversion of extender unit selectivity in the erythromycin polyketide synthase by acyltransferase domain engineering. *ACS Chem. Biol.* **2017**, *12* (1), 114−123.

(19) Li, Y.; Zhang, W.; Zhang, H.; Tian, W.; Wu, L.; Wang, S.; Zheng, M.; Zhang, J.; Sun, C.; Deng, Z.; Sun, Y.; Qu, X.; Zhou, J. Structural basis of a broadly selective acyltransferase from the polyketide synthase of splenocin. *Angew. Chem., Int. Ed.* **2018**, *57* (20), 5823−5827.

DOI: 10.1021/jacs.8b10521
J. Am. Chem. Soc. XXXX, XXX, XXX−XXX

(20) Del Vecchio, F.; Petkovic, H.; Kendrew, S. G.; Low, L.; Wilkinson, B.; Lill, R.; Cortes, J.; Rudd, B. A. M.; Staunton, J.; Leadlay, P. F. Active-site residue, domain and module swaps in modular polyketide synthases. *J. Ind. Microbiol. Biotechnol.* **2003**, *30* (8), 489−494.
(21) Koryakina, I.; McArthur, J. B.; Draelos, M. M.; Williams, G. J. Promiscuity of a modular polyketide synthase towards natural and non-natural extender units. *Org. Biomol. Chem.* **2013**, *11*, 4449−4458.
(22) Xue, Y.; Zhao, L.; Liu, H. W.; Sherman, D. H. A gene cluster for macrolide antibiotic biosynthesis in *Streptomyces venezuelae*: architecture of metabolic diversity. *Proc. Natl. Acad. Sci. U. S. A.* **1998**, *95* (21), 12111−6.
(23) Jung, W. S.; Kim, E.; Yoo, Y. J.; Ban, Y. H.; Kim, E. J.; Yoon, Y. J. Characterization and engineering of the ethylmalonyl-CoA pathway towards the improved heterologous production of polyketides in *Streptomyces venezuelae*. *Appl. Microbiol. Biotechnol.* **2014**, *98* (8), 3701−13.
(24) Bonnett, S. A.; Rath, C. M.; Shareef, A. R.; Joels, J. R.; Chemler, J. A.; Hakansson, K.; Reynolds, K.; Sherman, D. H. Acyl-CoA subunit selectivity in the pikromycin polyketide synthase PikAIV: steady-state kinetics and active-site occupancy analysis by FTICR-MS. *Chem. Biol.* **2011**, *18* (9), 1075−81.
(25) Kim, B. S.; Cropp, T. A.; Beck, B. J.; Sherman, D. H.; Reynolds, K. A. Biochemical evidence for an editing role of thioesterase II in the biosynthesis of the polyketide pikromycin. *J. Biol. Chem.* **2002**, *277* (50), 48028−34.
(26) Kalkreuter, E.; Williams, G. J. Engineering enzymatic assembly lines for the production of new antimicrobials. *Curr. Opin. Microbiol.* **2018**, *45*, 140−148.
(27) Hansen, D. A.; Koch, A. A.; Sherman, D. H. Identification of a thioesterase bottleneck in the pikromycin pathway through full-module processing of unnatural pentaketides. *J. Am. Chem. Soc.* **2017**, *139* (38), 13450−13455.
(28) Chemler, J. A.; Tripathi, A.; Hansen, D. A.; O'Neil-Johnson, M.; Williams, R. B.; Starks, C.; Park, S. R.; Sherman, D. H. Evolution of efficient modular polyketide synthases by homologous recombination. *J. Am. Chem. Soc.* **2015**, *137* (33), 10603−9.
(29) Pieper, R.; Gokhale, R. S.; Luo, G.; Cane, D. E.; Khosla, C. Purification and characterization of bimodular and trimodular derivatives of the erythromycin polyketide synthase. *Biochemistry* **1997**, *36* (7), 1846−51.
(30) Bycroft, M.; Weissman, K. J.; Staunton, J.; Leadlay, P. F. Efficient purification and kinetic characterization of a bimodular derivative of the erythromycin polyketide synthase. *Eur. J. Biochem.* **2000**, *267* (2), 520−6.
(31) Aldrich, C. C.; Beck, B. J.; Fecik, R. A.; Sherman, D. H. Biochemical investigation of pikromycin biosynthesis employing native penta- and hexaketide chain elongation intermediates. *J. Am. Chem. Soc.* **2005**, *127* (23), 8441−52.
(32) Mortison, J. D.; Kittendorf, J. D.; Sherman, D. H. Synthesis and biochemical analysis of complex chain-elongation intermediates for interrogation of molecular specificity in the erythromycin and pikromycin polyketide synthases. *J. Am. Chem. Soc.* **2009**, *131* (43), 15784−93.
(33) Yuzawa, S.; Deng, K.; Wang, G.; Baidoo, E. E.; Northen, T. R.; Adams, P. D.; Katz, L.; Keasling, J. D. Comprehensive in vitro analysis of acyltransferase domain exchanges in modular polyketide synthases and its application for short-chain ketone production. *ACS Synth. Biol.* **2017**, *6* (1), 139−147.
(34) Holzbaur, I. E.; Ranganathan, A.; Thomas, I. P.; Kearney, D. J.; Reather, J. A.; Rudd, B. A.; Staunton, J.; Leadlay, P. F. Molecular basis of Celmer's rules: role of the ketosynthase domain in epimerisation and demonstration that ketoreductase domains can have altered product specificity with unnatural substrates. *Chem. Biol.* **2001**, *8* (4), 329−340.
(35) Koch, A. A.; Hansen, D. A.; Shende, V. V.; Furan, L. R.; Houk, K. N.; Jimenez-Oses, G.; Sherman, D. H. A single active site mutation in the pikromycin thioesterase generates a more effective macrocyclization catalyst. *J. Am. Chem. Soc.* **2017**, *139* (38), 13456−13465.
(36) Smith, L.; Hong, H.; Spencer, J. B.; Leadlay, P. F. Analysis of specific mutants in the lasalocid gene cluster: evidence for enzymatic catalysis of a disfavoured polyether ring closure. *ChemBioChem* **2008**, *9* (18), 2967−2975.
(37) Menzella, H. G.; Reid, R.; Carney, J. R.; Chandran, S. S.; Reisinger, S. J.; Patel, K. G.; Hopwood, D. A.; Santi, D. V. Combinatorial polyketide biosynthesis by de novo design and rearrangement of modular polyketide synthase genes. *Nat. Biotechnol.* **2005**, *23* (9), 1171−1176.
(38) Lowry, B.; Li, X.; Robbins, T.; Cane, D. E.; Khosla, C. A Turnstile Mechanism for the Controlled Growth of Biosynthetic Intermediates on Assembly Line Polyketide Synthases. *ACS Cent. Sci.* **2016**, *2* (1), 14−20.
(39) Klaus, M.; Ostrowski, M. P.; Austerjost, J.; Robbins, T.; Lowry, B.; Cane, D. E.; Khosla, C. Protein-protein interactions, not substrate recognition, dominate the turnover of chimeric assembly line polyketide synthases. *J. Biol. Chem.* **2016**, *291* (31), 16404−15.
(40) Ruan, X.; Pereda, A.; Stassi, D. L.; Zeidner, D.; Summers, R. G.; Jackson, M.; Shivakumar, A.; Kakavas, S.; Staver, M. J.; Donadio, S.; Katz, L. Acyltransferase domain substitutions in erythromycin polyketide synthase yield novel erythromycin derivatives. *J. Bacteriol.* **1997**, *179* (20), 6416−25.
(41) Hans, M.; Hornung, A.; Dziarnowski, A.; Cane, D. E.; Khosla, C. Mechanistic analysis of acyl transferase domain exchange in polyketide synthase modules. *J. Am. Chem. Soc.* **2003**, *125* (18), 5366−5374.
(42) Patel, K.; Piagentini, M.; Rascher, A.; Tian, Z. Q.; Buchanan, G. O.; Regentin, R.; Hu, Z.; Hutchinson, C. R.; McDaniel, R. Engineered biosynthesis of geldanamycin analogs for Hsp90 inhibition. *Chem. Biol.* **2004**, *11* (12), 1625−33.
(43) Pfeifer, B. A.; Admiraal, S. J.; Gramajo, H.; Cane, D. E.; Khosla, C. Biosynthesis of complex polyketides in a metabolically engineered strain of *E. coli*. *Science* **2001**, *291* (5509), 1790−2.
(44) Zhang, Y. I-TASSER server for protein 3D structure prediction. *BMC Bioinf.* **2008**, *9*, 40.
(45) Roy, A.; Kucukural, A.; Zhang, Y. I-TASSER: a unified platform for automated protein structure and function prediction. *Nat. Protoc.* **2010**, *5* (4), 725−38.
(46) Yang, J.; Yan, R.; Roy, A.; Xu, D.; Poisson, J.; Zhang, Y. The I-TASSER Suite: protein structure and function prediction. *Nat. Methods* **2015**, *12* (1), 7−8.
(47) Humphrey, W.; Schulten, K.; Dalke, A. VMD - Visual Molecular Dynamics. *J. Mol. Graphics* **1996**, *14*, 33−38.
(48) Pettersen, E. F.; Goddard, T. D.; Huang, C. C.; Couch, G. S.; Greenblatt, D. M.; Meng, E. C.; Ferrin, T. E. UCSF Chimera–a visualization system for exploratory research and analysis. *J. Comput. Chem.* **2004**, *25* (13), 1605−1612.
(49) Sanner, M. F.; Olson, A. J.; Spehner, J. C. Reduced surface: an efficient way to compute molecular surfaces. *Biopolymers* **1996**, *38* (3), 305−320.
(50) Roe, D. R.; Cheatham, T. E., 3rd PTRAJ and CPPTRAJ: Software for processing and analysis of molecular dynamics trajectory data. *J. Chem. Theory Comput.* **2013**, *9* (7), 3084−95.
(51) Persistence of Vision Pty Ltd. *Persistence of Vision Raytracer* (Version 3.6); 2004.
(52) Case, D. A.; J, T. B., Betz, R. M.; Cerutti, D. S.; Cheatham, T. E., III; Darden, T. A.; Duke, R. E.; Giese, T. J.; Gohlke, H.; Goetz, A. W.; Homeyer, N.; Izadi, S.; Janowski, P.; Kaus, J.; Kovalenko, A.; Lee, T. S.; LeGrand, S.; Li, P.; Luchko, T.; Luo, R.; Madej, B.; Merz, K. M.; Monard, G.; Needham, P.; Nguyen, H.; Nguyen, H. T.; Omelyan, I.; Onufriev, A.; Roe, D. R.; Roitberg, A.; Salomon-Ferrer, R.; Simmerling, C. L.; Smith, W.; Swails, J.; Walker, R. C.; Wang, J.; Wolf, R. M.; Wu, X.; York, D. M.; Kollman, P. A. *AMBER 2015*; University of California: San Francisco, 2015.

DOI: 10.1021/jacs.8b10521
J. Am. Chem. Soc. XXXX, XXX, XXX−XXX